*Archives of Current Research International*

***Volume 24, Issue 1, Page 62-70, 2024; Article no.ACRI.111604***
***ISSN: 2454-7077***

# Crystallographic Benchmarking on Diffraction Pattern Profiling of Polymorphs-$TiO_2$ by WPPF for Pigment and Acrylic Paint

**Md. Mahmudul Kobir [a,b], Sumaya Tabassum [b,c], Shanawaz Ahmed [b], Sumaiya Islam Sadia [b] and Md. Ashraful Alam [b,c*]**

*[a] Asian Paints (Bangladesh) Limited, Bahadurpur, Gazipur-1703, Bangladesh.*
*[b] Department of Applied Chemistry and Chemical Engineering, Islamic University, Kushtia-7003, Bangladesh.*
*[c] Institute of Glass and Ceramic Research and Testing (IGCRT), Bangladesh Council of Scientific and Industrial Research (BCSIR), Dhaka-1205, Bangladesh.*

***Authors' contributions***

*This work was carried out in collaboration among all authors. All authors read and approved the final manuscript.*

***Article Information***

DOI: 10.9734/ACRI/2024/v24i1623

**Open Peer Review History:**
This journal follows the Advanced Open Peer Review policy. Identity of the Reviewers, Editor(s) and additional Reviewers, peer review comments, different versions of the manuscript, comments of the editors, etc are available here: https://www.sdiarticle5.com/review-history/111604

***Original Research Article***

***Received: 11/11/2023***
***Accepted: 16/01/2024***
***Published: 22/01/2024***

## ABSTRACT

At a very low temperature high crystalline phase of $TiO_2$ best-fitted strain anatase was synthesized by peptization which was the prime object of this study. Unresolved parameters were investigated by the X-ray diffraction (XRD) technique employed for lattice parameters, crystallite size, lattice volume, strain, crystal structure, d-spacing and percentage of phase in weight fraction. 54.40 % anatase, 29.10 % brookite and 16.50 % rutile crystalline phase were found by whole powder

**Corresponding author: Email: ashrafulalam@bcsir.gov.bd;*

pattern fitting (WPPF-Rietveld's refinement) method and lattice volume of anatase 137.150, brookite 267.079 and rutile 62.901 Å³ as well the crystal strain 0.307, 0.45 and 0.28 % of anatase, brookite and rutile polymorph-$TiO_2$ found respectively. The calculated lattice parameters of the anatase are $\alpha=\beta=\gamma=$ 90.0°; a=b= 3.8056 Å, c= 9.470 Å and predominant (101), (004) and (200) miller indices with diffracted angle (2Ɵ) 25.38, 37.26 and 48.22 observed. The average crystallite size was 7.39 nm which confirmed the formation of nano-crystal-$TiO_2$ due to the highly dispersed on medium. The percentage of strain of the individual polymorphs of $TiO_2$ shows the best fit used for the pigment and acrylic paint.

*Keywords: Acrylic paint; Anatase; Brookite; Pigment; Rutile.*

## 1. INTRODUCTION

Pablo Picasso turned forty in 1921, and not long after an industrial process for making titanium white pigment was created and made public [1]. He has been employing titanium white as a photocatalyst in his work [2] which might seriously harm his reputation and he wasn't the only one [1]. Apart from its application in paintings [3-6], titanium white has also been included in plastic art pieces and photographic paper (resin-coated prints), resulting in issues with deterioration [7,8]. An established photocatalyst is titanium dioxide. A series of reactions may result in the creation of radicals when titanium dioxide absorbs UV light. These free radicals can damage nearby pigment which can lead to an organic medium breakdown and embrittlement, gloss loss or chalking. The colour may also change when dye-stuffs, pigments or colourants are used [9–11]. Pigments made of titanium dioxide have been appropriately used to give a variety of materials opacity or whiteness. Various sectors, including plastics, paints, paper and inks can utilize them [12]. Because of its high refractive index and capacity to absorb UV radiation, $TiO_2$ has several remarkable properties that have earned it an exceptional reputation among other white pigments. These advantages include effective light scattering and product durability. Additionally, because it is non-toxic there is less risk to safety and health, making it suitable for use in a variety of applications [13]. $TiO_2$ nanoparticles exhibit distinct optical behaviours in comparison to traditional $TiO_2$ pigments. $TiO_2$ nanoparticle optical characteristics are explained by the Rayleigh theory of light scattering. Small particles more effectively scatter light at shorter wavelengths, according to this theory. Additionally, the anatase form of $TiO_2$ nanoparticle photocatalytic activity has been used to create a variety of materials with the self-cleaning feature [14]. The industry has paid a lot of attention lately to self-cleaning coatings that use photocatalytic titanium dioxide nanoparticles. $TiO_2$ nanoparticles have a strong oxidation capacity that can be utilized to eradicate dirt stains or kill bacteria that have adhered to the walls. Moreover, when such a coating is put on external surfaces, the super-hydrophilic nature of dirt and stains can make it simple for water or rainfall to wash them away [15,16]. Because of their incredibly high surface area to particle size ratio, nanoparticles also have a strong potential to agglomerate as well as magnetic and nanorod properties [17-19]. Thus, dispersing the nanoparticles without agglomerating in the organic binders is essential for creating an appropriate $TiO_2$-modified paint. The surfaces of the $TiO_2$ nanoparticles are coated with sufficient precipitated inorganic compounds, such as $SiO_2$ and $Al_2O_3$, to enhance their dispersion and decrease their photoactivity [16]. The crystalline phase percentage of nanomaterials is also effective to their inherent property [20-23] Commercially obtainable three $TiO_2$ nanoparticles have been used as additions in varying quantities to white acrylic water-based paint to study how this improves the paint's ability to clean itself. For the preparation of the polymorphs $TiO_2$, a different route is also applied such as peptization [24], hydrothermal or solvothermal [25,26], sol-gel [27], etc are followed. The primary focus of this study is the ultrafine highly crystalline polymorph-$TiO_2$ synthesized in the forms of rutile, brookite and anatase by a unique simple route.

## 2. MATERIALS AND METHOD

Titanium isopropoxide (TTIP), Ethanol, Nitric acid and Isopropyl alcohol (IP) are purchased from Sigma-Aldrich and De-ionized water is collected from IPCRD, IGCRT, BCSIR. The precursor solution TTIP and IP was mixed with a 1: 3 ratio (v/v) and stirred for 10.00 minutes. On another 500.00 ml beaker add 250.00 ml DI water and maintain pH for 2.0 to 2.5. The prepared two solutions were mixed with and followed the 400.00 rpm and 65 ◦C for 17-18.0 h peptization of the gel was formed. After the peptization, the

gel volume decreases to 50.0 $cm^3$. The final suspension was washed with ethanol with centrifuged at 8000.00 rpm several times. The precipitated dried at oven 60.0 °C a white fine powder was obtained. After preparing the sample at 9.0 hours the crystallographic measurement techniques were employed at room temperature.

## 3. CHARACTERIZATION

The Smart-Lab SE, a versatile X-ray Diffractometer manufactured by Rigaku in Japan was used to observe X-ray diffraction patterns. The instrument was equipped with a 40 KV x 50 mA (2.00 kW) source, 10.00mm CBO-BB optics, and a $K_\beta$ filter made of Ni (28). In this case, the procedure was executed with a step size of $0.001^0$ (speed of $05^0$/min), a HyPix-400 (HPAD-1D) detector operating in standard mode and collecting $10^6$/pixel rate data. The crystallographic structure and lattice parameters of a material are ascertained by subjecting the material to irradiation with incoming X-rays and subsequently measuring the diffraction angles and intensities of the X-rays that exit the material [28]. The analysis was conducted on the powdered material at a temperature of 25.00 ℃, which corresponds to room temperature. X-ray diffraction is commonly used to determine the crystal structure of polymorph-$TiO_2$. The Debye-Scherrer formula has been utilized to determine the size of crystallites by X-ray diffraction examination.

$$D = \frac{0.9\lambda}{\beta cos\theta}$$

Where, D = Crystal size, λ = Wavelength of the X-ray (λ=0.1541 nm), β = Full width at half maximum and θ = Diffraction angle [24].

Bragg`s law has been applied for the determination of the d-spacing values (inter-planar distance between atoms)

$$d = \frac{\lambda}{2sin\theta}$$

Table 1 is utilized for the listing of the crystal size and d-spacing values that are determined. The quantitative analysis of the synthesized powder-$TiO_2$ was determined using the WPPF technique (Whole powder pattern fitting method) given in Table 6.

## 4. RESULTS AND DISCUSSION

The X-ray crystallographic diffractogram revealed three prominent diffractions at 2Ɵ= 25.38, 37.26 and 48.22 with corresponding intensities of 3927, 554 and 927 counts per second (cps). On the other hand, two minor diffractions were also observed at 2Ɵ= 30.65 and 54.5 with intensities of 227 and 801 cps. The main three diffractions 25.38, 37.26 and 48.22 were responsible for anatase-$TiO_2$ [ICDD Card No # 01-083-5914] and another two diffractions 30.65 and 54.5 were responsible for brookite and rutile-$TiO_2$ polymorphs respectively which as shown in Fig. 1.

The minor diffraction was found at 2Ɵ= 63.41, 69.43 and 75.73 with intensity of 457, 76 and 58 cps which is also responsible for the prominent anatase [ICDD Card No # 01-083-5914].

Table 1, shows that the three main diffractions were observed at 25.38, 37.26 and 48.22 with the prominent respective Miller indices (101), (004) and (200). The crystallite size was determined by the Debye-Scherrer formula with three respective diffractions such as 5.87, 11.20 and 5.08 nm. The calculated average crystallite size was 7.39 nm which confirmed the formation of nanocrystal-$TiO_2$ that shows an outstanding dispersion on paint medium [12]. The interplanar distance (d-spacing) was also calculated by the Bragg formula of the main three intense diffractions. The calculated d-spacing at 25.38, 37.26 and 48.22 were 0.35056, 0.24110 and 0.18858 nm. This d-spacing exhibits the uniformity of the nanocrystal-$TiO_2$ [24,23,29].

**Table 1. The calculation of the grain size of $TiO_2$**

| Diffraction angle (2Ɵ) | Theta (Ɵ) | (h k l) | FWHM (radians) | Size of the crystallite (D ± 0.01) nm | d-spacing (d ± 0.001) (nm) |
|---|---|---|---|---|---|
| 25.38 | 12.69 | (1 0 1) | 1.453 | 5.87 | 0.35056 |
| 37.26 | 18.63 | (0 0 4) | 0.79 | 11.20 | 0.24110 |
| 48.22 | 24.11 | (2 0 0) | 1.792 | 5.08 | 0.18858 |

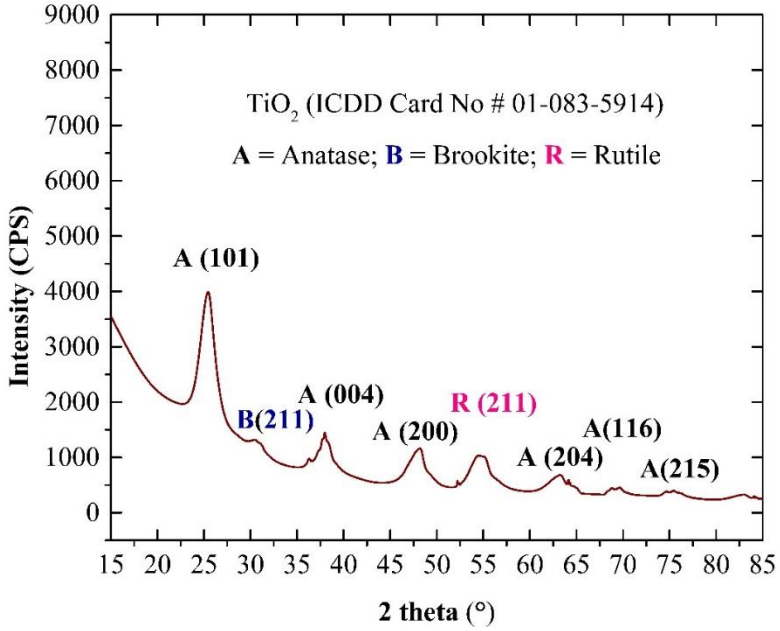


**Fig. 1. X-ray diffractogram of synthesized $TiO_2$ at room temperature**

**Table 2. Peak profiling of $TiO_2$ by diffraction angle**

| Diffraction angle (2Θ) | Theta (Θ) | 1000× $Sin^2Θ$ | Reflection | Remarks |
|---|---|---|---|---|
| 25.38 | 12.69 | 48.25 | (1 0 1) | $1^2 + 0^2 + 1^2 = 2$ |
| 37.26 | 18.63 | 102.05 | (0 0 4) | $0^2 + 0^2 + 4^2 = 16$ |
| 48.22 | 24.11 | 166.863 | (2 0 0) | $2^2 + 0^2 + 0^2 = 4$ |

Table 2, exhibits the peak profiling of the $TiO_2$ by diffraction position (Θ). Three significant values of the peak profiling were 48.25, 102.50 and 166.83 observed at the 2Θ= 25.38, 37.26 and 48.22. The peak profiling and remarks value interval also ensured the particles were uniformly distributed onto the plane into the crystal system [24,23,30].

Table 3, exhibits the peak profiling of the $TiO_2$ by d-spacing. The peak profiling was 81.37, 172.05 and 281.21 observed at the 2Θ= 25.38, 37.26 and 48.22 values with respective d-spacing 3.5056, 2.4110 and 1.8858 Å. Three significant interval values from peak profiling ensure that the crystals are well-growth onto plane [24] for their uniform distribution as well as remarks value.

**Table 3. Peak profiling of $TiO_2$ by inter-planner (d-spacing) distance**

| Diffraction angle (2Θ) | Inter-planner distance (d), (Å) | $1000/d^2$ | Reflection | Remarks |
|---|---|---|---|---|
| 25.38 | 3.5056 | 81.37 | (1 0 1) | $1^2 + 0^2 + 1^2 = 2$ |
| 37.26 | 2.4110 | 172.05 | (0 0 4) | $0^2 + 0^2 + 4^2 = 16$ |
| 48.22 | 1.8858 | 281.21 | (2 0 0) | $2^2 + 0^2 + 0^2 = 4$ |

**Table 4. An analysis of the experimental (Exp.) and standard (Std.) diffraction data is being conducted for comparison**

| Diffraction angle (2Θ) | | Inter-planer distance (d) (Å) | | Lattice parameters of Std. |
|---|---|---|---|---|
| (Exp.) | (Std.) | (Exp.) | (Std.) | Space Group: I41/amd (141) |
| 25.38 | 25.307 | 3.5056 | 3.516360 | a=b= 3.7845 Å c= 9.5111 Å; |
| 37.26 | 37.804 | 2.4110 | 2.377780 | α=β=γ=90.0°; c/a: 2.513, |
| 48.22 | 48.042 | 1.8858 | 1.892250 | Volume= 136.22 Å³. |
| | | | | [ICDD Card No # 01-083-5914] |

Table 4, displays the comparison between experimental data and standard data from ICDD (Card No # 01-083-5914). The standard diffractions were detected at 25.307, 37.804 and 48.042 whereas the synthesis $TiO_2$ diffraction was seen at 2Θ= 25.38, 37.26 and 48.22 which closely matches the standard data. The ICDD bilographic shown as Space Group: I41/amd (141) a=b= 3.7845 Å c= 9.5111 Å; α=β=γ=90.0°; c/a: 2.513, Volume= 136.22 Å. Alternatively, the d-spacing values of the standard data were observed at 3.516360, 2.377780 and 1.892250 Å which is also similar to the synthesized $TiO_2$ d-spacing 3.5056, 2.4110 and 1.8858 Å.

Table 5, represents the normalized intensity (I.) of the synthesized $TiO_2$ and ICDD standard. The I. calculated values of synthesized $TiO_2$ were 100.00, 14.0 and 72.00 at the diffraction position 2Θ= 25.38, 37.26 and 48.22. So, the crystallinity was observed at 53.80% whereas the ICDD standard shows the crystallinity at 70.20% confirming that it is the highly ordered [24] in a three-dimensional lattice.

**Table 5. Calculation of percentage of Crystallinity**

| 2Θ (Exp.) | Norm. I. (%) (Exp.) | Percent of Crystallinity (%) | 2Θ (Std.) | Norm. I. (%) (Std.) | Percent of Crystallinity (%) |
|---|---|---|---|---|---|
| 25.38 | 100.00 | | 25.307 | 100.00 | |
| 37.26 | 14.00 | 53.80 | 37.804 | 18.00 | 70.20 |
| 48.22 | 72.00 | | 48.042 | 24.50 | |

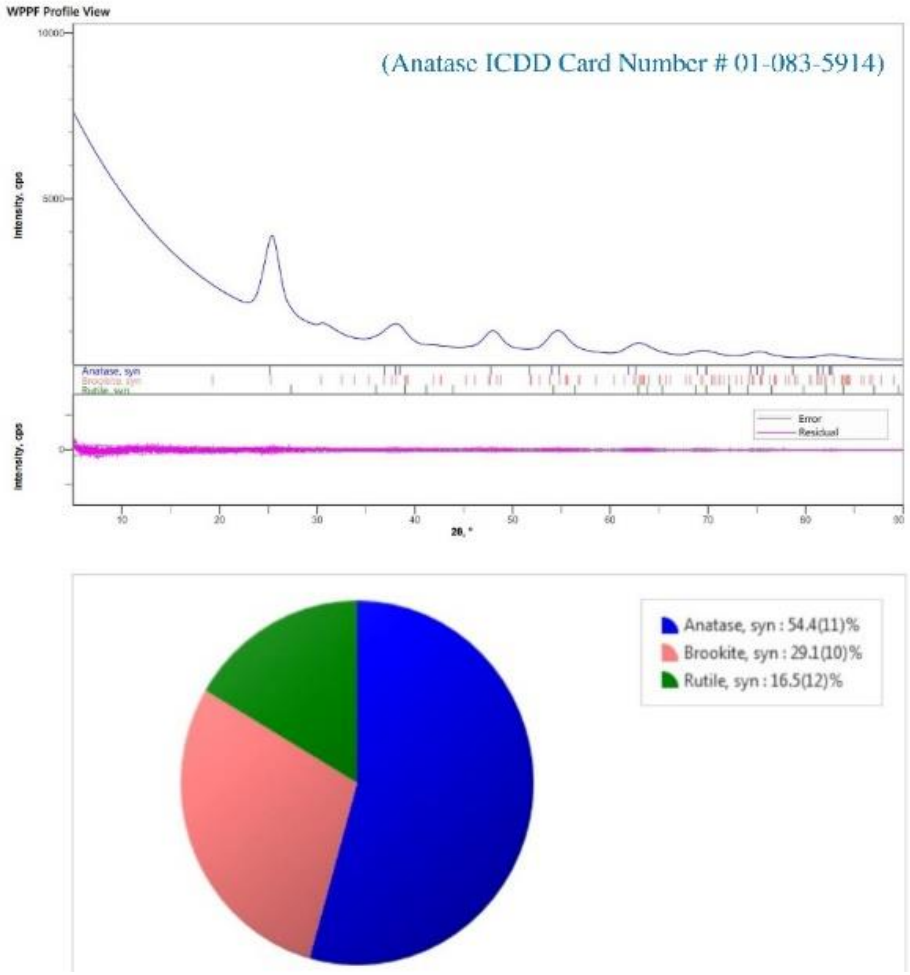


**Fig. 2. Quantitative analysis of Polymorph-$TiO_2$ by the WPPF (Whole powder pattern fitting) method**

Fig. 2, Shows the phase percentage (%) of the crystalline polymorphs of $TiO_2$ that is determined by the WPPF method. The calculated phase percentage observed that 54.40% anatase, 29.10% brookite and 16.50% rutile were found at the pattern fitting condition Rwp, 9.84%, Rp 7.01%, S 0.4092, $\chi^2$ 0.1674.

Table 6, shows the Rietveld refinement of the polymorph-$TiO_2$ at the same pattern-fitting condition whereas the calculated lattice volume of anatase 137.150, brookite 267.079 and rutile 62.901 $Å^3$ as well as the crystal strain 0.307, 0.45 and 0.28% of anatase, brookite and rutile polymorph respectively. The strain ensured that the stability of crystalline polymorph-$TiO_2$ was suitable for the paint medium. The crystal lattice parameters are also calculated by Rietveld refinement, whereas anatase $\alpha=\beta=\gamma=90.0°$, a=b=3.8056 Å, c=9.470 Å; brookite $\alpha=\beta=\gamma=90.0°$, a=9.186 Å b=5.500 Å, c=5.287 Å; rutile $\alpha=\beta=\gamma=90.0°$, a=b=4.613 Å, c=2.956 Å; for its fitted data confirmed the uniformity of the crystal are best suitable to the UV and other radiation that was various prominent application for the pigment and acrylic paint.

Fig. 3, strain curve shows that the high strain easily decomposed the preferred orientation (001) and turned into an amorphous [31]; the anatase strain (0.307 %) curve is more stable than brookite (0.45%) cure as well as rutile. So, the anatase strain is preferred to the paint for its antimicrobial and light scattering properties as well as self-cleaning for the rutile polymorph strain [32]. The application of $TiO_2$ coating is

**Table 6. Rietveld's refinement of the polymorph-$TiO_2$ by WPPF**

| Rwp (%) | Rp (%) and S | Weight fraction, Wt (± 0.01) % | Lattice volume (± 0.01) $Å^3$ | Strain (± 0.001) % | Lattice parameters |
|---|---|---|---|---|---|
| | | | **Anatase** | | |
| 9.84 | 7.01<br>0.4092 | 54.40 | 137.150 | 0.307 | $\alpha=\beta=\gamma=$ 90.0 °<br>a=b= 3.8056Å, c= 9.470Å |
| | | | **Brookite** | | |
| 9.84 | 7.01<br>0.4092 | 29.1 | 267.079 | 0.45 | $\alpha=\beta=\gamma=$ 90.0 °<br>a= 9.186 Å, b=5.500 Å,<br>c= 5.287 Å |
| | | | **Rutile** | | |
| 9.84 | 7.01<br>0.4092 | 16.50 | 62.901 | 0.28 | $\alpha=\beta=\gamma=$ 90.0 °<br>a=b= 4.613 Å, c= 2.956 Å |

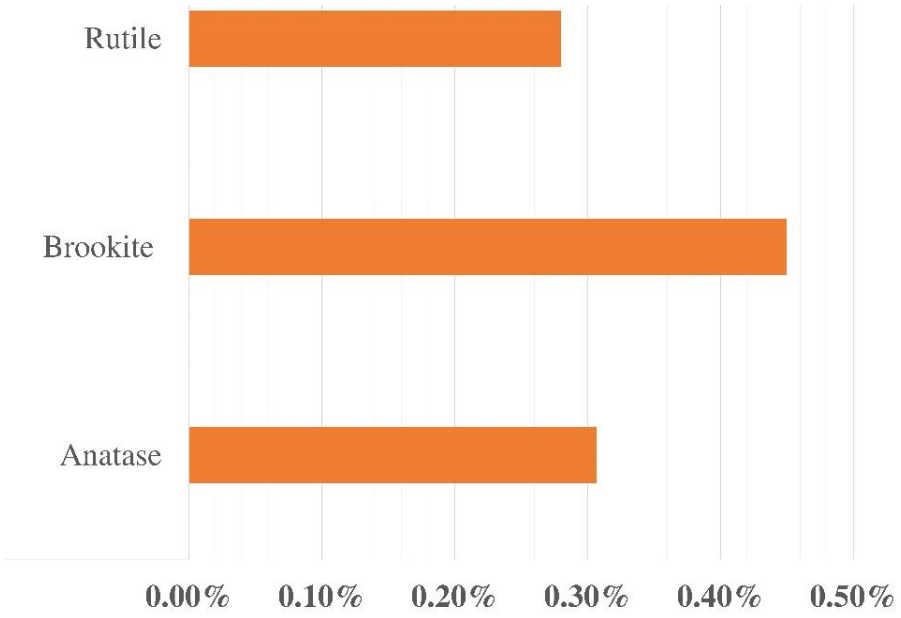


**Fig. 3. Strain curve of polymorph-$TiO_2$**

possible on various surfaces including the surface of indoor and outdoor buildings, metallic objects, wooden frames and domestic and professional instruments [33]. Rutile and anatase are the two polymorphs of $TiO_2$ but the rutile form of $TiO_2$ cannot boost implemented photocatalytic activity [33,34]. On the contrary, the anatase prominent phase form can enhance the photocatalytic activity when mixed with paint as well as film formation, increasing coverage area, hiding, smooth surface area and structural modification due to its contrast ratio, opacity, refractive index and viscosity [35-37,32,19]. The addition of $TiO_2$ into the paint can modify the paint performance traits including peeling, wake retention, cracking, flaking and muckraking [38]. Moreover, $TiO_2$ can enhance opacity and brightness and it can improve the durability of the paint [39,25]. $TiO_2$ is a widely known pigment because of its identical properties (including inert, stable, less costly and non-toxic) [40]. As an exceptional UV light absorber, $TiO_2$ defenses from damage that occurs due to UV radiation [39,41]. Because of the identical features of $TiO_2$, medicinal products with very minute concentrations of pigment can reveal appealing shades and distinctive characteristics [40]. For tinting a variety of products in the cosmetics and pharmaceutical industries, $TiO_2$ is extensively used as a pigment [40,42,31]. Across this industry, $TiO_2$ is employed to produce several products including lotions, shampoos, sunscreens, toothpaste and so on [43]. The prepared sample might be used for the pigments as well as for acrylic paint.

## 5. CONCLUSION

High crystalline phase 54.40% $TiO_2$ best-fitted strain anatase was synthesized at a very low temperature 60.0 °C. Exhaustive parameters were investigated by X-ray diffraction (XRD) techniques employed for lattice parameters, crystal size, lattice volume, strain and weight fraction. 54.40% anatase, 29.10% brookite and 16.50% rutile were found by WPPF method and lattice volume of anatase 137.150, brookite 267.079 and rutile 62.901 Å$^3$ as well the crystal strain 0.307, 0.45 and 0.28% of anatase, brookite and rutile polymorph observed respectively. The strain of the individual polymorphs of $TiO_2$ show best-fitted used for the pigment and acrylic paint for its preferred orientation. The average crystallite size was 7.39 nm which confirmed the formation of nanocrystal-$TiO_2$ and uniformly distribution into the medium. For the outstanding significant properties of the $TiO_2$ polymorphs it could be very useful materials for the paint, wallpaper, colour-bank and pigment etc. industry.

## ACKNOWLEDGEMENT

The author's heartiest thanks to IPCRD, IGCRT, Division in Charge for using the software and computers.

## COMPETING INTERESTS

The authors have declared that no competing interests exist.

## REFERENCES

1. Laver M. Chapter 10: titanium white, in: E.W. Fitzhugh (Ed.), Artists' Pigments: A Handbook of their History and Characteristics, National Gallery of Art. 1997;3:295-355.
   Available:http://dx.doi.org/10.2307/1506685.
2. Du P, Bueno-Lopez A, Verbaas M, Almeida AR, Makkee M, Moulijn JA, Mul G. The effect of surface OH-population on the photocatalytic activity of rare earth-doped P25-TiO2 in methylene blue degradation. Journal of Catalysis. 2008; 260(1):75-80.
3. de Keijzer M, de Groot S, Megens L, Van Keulen H. Schildertechnisch onderzoek aan Mondriaans Compositie met rood, zwart, geel en grijs uit 1920. Unpublished results. Instituut Collectie Nederland; 2008.
4. de Keijzer M. The colourful twentieth century, in S. Fairbrass, J. Hermans (Eds.), Modern Art: The Restoration and Techniques of Modern Paper and Paints, United Kingdom Institute of Conservation. 1989;13–20.
   ISBN: 1871656044.
5. Van Driel BA, Kooyman PJ, Van den Berg KJ, Schmidt-Ott A, Dik J. A quick assessment of the photocatalytic activity of TiO2 pigments—From lab to conservation studio! Microchemical Journal. 2016;126: 162-171.
6. de Keijzer M. The history of modern synthetic inorganic and organic artists' pigments, in: J.A. Mosk, N.H. Tennent (Eds.), Contributions to Conservation: Research in Conservation at the Netherlands Institute for Cultural Heritage, James & James (Science Publishers) Ltd; 2002.
   ISBN: 1-902916-09-3.

7. van Oosten TB, I Fundeanu, C Bollard, Castro C d, A Lagana. Lights out! The conservation of polypropylene wall tapestries, in B. Keneghan, L. Egan (Eds.), Plastics. Looking to the Future and Learning from the Past, Archetype Books; 2008.
ISBN: 1904982433.
8. Parsons TF, Gray GG, Crawford IH. To RC or not to RC, J. Appl. Photogr. Eng. 1979;5(2):110–117.
9. Völz Hans G, Kaempf G, Fitzky Hans G, Klaeren A. The chemical nature of chalking in the presence of titanium dioxide pigments, in: F.H. Winslow (Ed.), Photodegradation and Photostabilization of Coatings, ACS Symposium Series, American Chemical Society. 1981;151: 163–182.
10. Egerton TA, King CJ.,The influence of light intensity on photoactivity in $TiO_2$ pigmented systems, J. Oil Col. Chem. Assoc. 1979; 62:386–391.
11. Allen NS, Edge M, Ortega A, Sandoval G, Liauw CM, Verran J, et al. Degradation and stabilisation of polymers and coatings: Nano versus pigmentary titania particles. Polymer Degradation and Stability. 2004;85(3):927-946.
12. Khataee A, Mansoori GA. Nanostructured titanium dioxide materials: properties, preparation and applications. World Scientific; 2011.
13. Jana NR, Gearheart L, Murphy CJ. Seed-mediated growth approach for shape-controlled synthesis of spheroidal and rod-like gold nanoparticles using a surfactant template. Advanced Materials. 2001;13(18):1389-1393.
14. Folli A, Pade C, Hansen TB, De Marco T, Macphee DE. TiO2 photocatalysis in cementitious systems: Insights into self-cleaning and de-pollution chemistry. Cement and Concrete Research. 2012; 42(3):539-548.
15. Gunschera J, Markewitz D, Bansen B, Salthammer T, Ding H. Portable photocatalytic air cleaners: Efficiencies and by-product generation. Environmental Science and Pollution Research. 2016;23: 7482-7493.
16. Subbiah G, Premanathan M, Kim SJ, Krishnamoorthy K, Jeyasubramanian K. Preparation of TiO2 nano paint using ball milling process and investigation on its antibacterial properties. Materials Express. 2014;4(5):393-399.
17. Govind B, Bharti P, Srivastava M, Kumar A, Bano S, Bhatt K, et al. Magnetic properties of intermediate Ni2-xMn1+ xSb full-Heusler compounds. Materials Research Bulletin. 2021;142: 111427.
18. Govind B, Srivastava M, Pulikkotil JJ, Misra DK. Electronic structure and magnetic properties of a full-Heusler Mn2NiSb: Cu2MnAl type structure. Journal of Magnetism and Magnetic Materials. 2021;517:167375.
19. Qin, DD, Bi YP, Feng XJ, Wang W, Barber GD, Wang T, et al. Hydrothermal growth and photoelectrochemistry of highly oriented, crystalline anatase TiO2 nanorods on transparent conducting electrodes. Chemistry of Materials. 2015; 27(12):4180-4183.
20. Alam MA, Munni SA, Mostafa S, Bishwas RK, Jahan SA. An Investigation on Synthesis of Silver Nanoparticles. Asian Journal of Research in Biochemistry. 2023; 12(3):1-10.
21. Alam MA, Mobashsara MT, Sabrina SM, Bishwas RKB, Debasish DS, Shirin SAJ. One-pot Low-Temperature Synthesis of High Crystalline Cu Nanoparticles. Malaysian Journal of Science and Advanced Technology. 2023;122-127.
22. Alam MA, Tabassum M, Mostofa S, Bishwas RK, Sarkar D, Jahan SA. The effect of precursor concentration on the crystallinity synchronization of synthesized copper nanoparticles. Journal of Crystal Growth. 2023;621:127386.
23. Tabassum M, Alam MA, Mostofa S, Bishwas RK, Sarkar D, Jahan SA. Synthesis and crystallinity integration of copper nanoparticles by reaction medium. Journal of Crystal Growth. 2024;626: 127486.
24. Alam MA, Bishwas RK, Mostofa S, Jahan SA. Low-temperature synthesis and crystal growth behavior of nanocrystal anatase-TiO2. Materials Letters. 2024;354:135396.
25. Gupta T, Cho J, Prakash J. Hydrothermal synthesis of TiO2 nanorods: formation chemistry, growth mechanism, and tailoring of surface properties for photocatalytic activities. Materials Today Chemistry. 2021;20:100428.
26. Saqib M, Rahman N, Safeen K, Mekkey SD, Salem MA, Safeen A, et al. Structure phase-induced photodegradation properties of cobalt-sulfur co-doped TiO2 nanoparticles synthesized by hydrothermal

route. Journal of Materials Research and Technology. 2023;26:8048-8060.
27. Sharma A, Karn RK, Pandiyan SK. Synthesis of TiO2 nanoparticles by sol-gel method and their characterization. J Basic Appl Eng Res. 2014;1(9):1-5.
28. Rahman MM, Maniruzzaman M, Yeasmin MS, Gafur MA, Shaikh MAA, Alam MA, et al. Adsorptive abatement of Pb2+ and crystal violet using chitosan-modified coal nanocomposites: A down flow column study. Groundwater for Sustainable Development. 2023;23:101028.
29. Moulick SP, Hossain MS, Al Mamun MZU, Jahan F, Ahmed MF, Sathee RA, et al. Characterization of waste fish bones (*Heteropneustes fossilis* and *Otolithoides pama*) for photocatalytic degradation of Congo red dye. Results in Engineering. 2023;20:101418.
30. Bishwas RK, Mostofa S, Alam MA, Jahan SA. Removal of malachite green dye by sodium dodecyl sulfate modified bentonite clay: Kinetics, thermodynamics and isotherm modeling. Next Nanotechnology. 2023;3:100021.
31. Zhang Y, Liu Z, Zhang X, Wang Q, Wang Q, Wang H, et al. The formation mechanism of (001) preferred orientation for anatase TiO2 film prepared by DC pulsed magnetron sputtering. Vacuum. 2021;190:110287.
32. Ramadan M, Kohail M, Abadel AA, Alharbi YR, Soliman AM, Mohsen A. Exploration of mechanical performance, porous structure, and self-cleaning behavior for hydrothermally cured sustainable cementitious composites containing de-aluminated metakaolin waste and TiO2 nanoparticles. Journal of Materials Research and Technology; 2023.
33. Braun JH, Baidins A, Marganski RE. TiO2 pigment technology: a review Progress in Organic Coatings. 1992;20:105–38.
34. Luttrell T, Halpegamage S, Tao J, Kramer A, Sutter E, Batzill M. Why is anatase a better photocatalyst than rutile? - Model studies on epitaxial TiO2 films Sci Rep. 2014;4:4043.
35. Liu K, Cao M, Fujishima A, Jiang L. Bio-Inspired Titanium Dioxide Materials with Special Wettability and their Applications Chemical Reviews. 2014;114.
36. Lied E, Morejon C, Basso R, Trevisan A, Bittencourt P, Fronza F. Photocatalytic degradation of H 2 S in the gas-phase using a continuous flow reactor coated with TiO 2 -based acrylic paint Environmental Technology. 2018;40:1–24.
37. Fujishima A, Zhang X, Tryk D. TiO2 Photocatalysis and Related Surface Phenomena Surface Science Reports. 2008;63:515–82.
38. Basso A, Battisti A P, Moreira R de F P M, José H J. Photocatalytic effect of addition of TiO2 to acrylic-based paint for passive toluene degradation* Environmental Technology. 2020;41:1568–79.
39. Diebold M. Optimizing the benefits of TiO2 in paints Journal of Coatings Technology and Research. 2019;17.
40. Wu X. Applications of Titanium Dioxide Materials Titanium Dioxide - Advances and Applications (IntechOpen); 2021.
41. Anon Titanium Dioxide - an overview | ScienceDirect Topics.
42. Lakshmanan V, Bhowmick A, Halim A. Titanium Dioxide - Production, Properties and Applications. 2014;75.
43. Anon Titanium Dioxide: Chemical Properties, Applications and Environmental Effects – Nova Science Publishers.



*Peer-review history:*
*The peer review history for this paper can be accessed here:*
*https://www.sdiarticle5.com/review-history/111604*